

Resonant Ultrasound Spectroscopy of single crystalline KH_2PO_4

Vikram Singh^{a,*}, M. Bicky Singh^{a,*}, Sunil Nair^{a,**}

^aDepartment of Physics, Indian Institute of Science Education and Research, Dr. Homi Bhabha Road, Pune 411008, India

Abstract

This study employs resonant ultrasound spectroscopy (RUS) to investigate the elastic properties of single crystalline KH_2PO_4 (KDP) through the paraelectric to ferroelectric phase transition. Noteworthy anomalies are observed in selected resonance modes and their corresponding mechanical quality factors (Q) around the transition temperature. The thermal evolution of elastic constants (C_{ij}) across the phase transition reveals a significant softening of C_{11} , C_{12} , and C_{13} , accompanied by a stiffening in C_{66} . Additionally, both C_{33} and C_{44} exhibit a minimum value at the transition. This anomalous behavior of all elastic constants (C_{ij}) across the phase transition suggests the involvement of higher-order coupling between the lattice and polarization in the KDP crystal. Furthermore, the bulk modulus (B) undergoes a sudden softening precisely at the transition, while the shear modulus (G) initially softens and subsequently stiffens across the transition.

Keywords: Ferroelectric, KH_2PO_4 (KDP), Phase transition, Elastic constants, Resonant Ultrasound Spectroscopy.

1. Introduction

Potassium dihydrogen phosphate (KH_2PO_4), commonly referred to as KDP, is a well-known dielectric material widely utilized in non-linear optical and electro-optical applications [1, 2, 3]. KDP undergoes a paraelectric to ferroelectric phase transition ($T_C \sim 122$ K) accompanied by a tetragonal (space group $I\bar{4}2d$) to orthorhombic ($Fdd2$) crystal symmetry change [4, 5, 6]. This phase transition has been a subject of interest for a long time, with some reports suggesting its proximity to a tricritical point [4, 7, 8, 9, 10, 11, 12]. The phase transition in KDP has been attributed to changes in hydrogen bonding, leading to an abrupt jump in both the polarization and lattice parameters. This strong coupling between the lattice and polarization in this material has prompted extensive investigations into its elastic properties. The elastic properties have been probed using various acoustic techniques, including pulse-echo ultrasonic scattering, Brillouin scattering, and resonance frequency measurements [13, 14, 15, 16, 17, 12]. These techniques possess certain advantages and experimental constraints, such as the frequency range, sample size, and crystal orientation. As a result, they may yield different values for the elastic constants. Initial investigation using ultrasonic experiments on KDP unveiled anomalous behavior in the elastic constants C_{33} and C_{66} across the phase transition, which was attributed to strong piezoelectric coupling [15, 17, 13]. Furthermore, a recent study has also revealed anomalies in other longitudinal elastic constants, including C_{11} , C_{44} , C_{33} and C_{66} across the transition [12]. However, the aspect of crystal symmetry change at the transition has not been taken into account

in these ultrasonic experiments. In KDP crystal, the tetragonal crystal symmetry ($\bar{4}2m$) consists of six elastic constants, while the orthorhombic symmetry ($2mm$) encompasses nine elastic constants. The evolution of the additional elastic constants in the low symmetry phase remain to be explored.

In this context, resonant ultrasound spectroscopy (RUS) has emerged as a compelling technique for the determination of elastic constants [18, 19, 20, 21, 22, 23, 24]. Unlike conventional ultrasonic methods, RUS enables the simultaneous measurement of all elastic constants within a single scan, providing a comprehensive characterization of a solid's elastic behavior. Moreover, the inverse of the mechanical quality factor Q^{-1} obtained from RUS measurements offers insights into elastic relaxation phenomena [25]. Given that RUS is highly sensitive to crystal symmetry and provides a comprehensive set of elastic constants, it would be intriguing to investigate the thermal behavior of all the elastic constants of KDP crystal across the phase transition. To the best of our knowledge, RUS has solely been carried out on KDP at room temperature till date [26].

In the present study, we conducted temperature-dependent RUS measurements on high-quality KDP single crystal within the temperature range of 100 K to 300 K. The results revealed a systematic elastic softening across the entire temperature range, except in the transition region where pronounced stiffness was observed near the transition temperature. The phase transition is effectively probed using the RUS data, as evidenced by the distinct patterns observed in the f_0^2 and Q^{-1} plots. Additionally, anomalous behavior across in the all elastic constants further indicates the presence of a complex higher order piezoelectric coupling across the phase transition in KDP crystal.

* Authors contributed equally

** Corresponding author

Email address: sunil@iiserpune.ac.in (Sunil Nair)

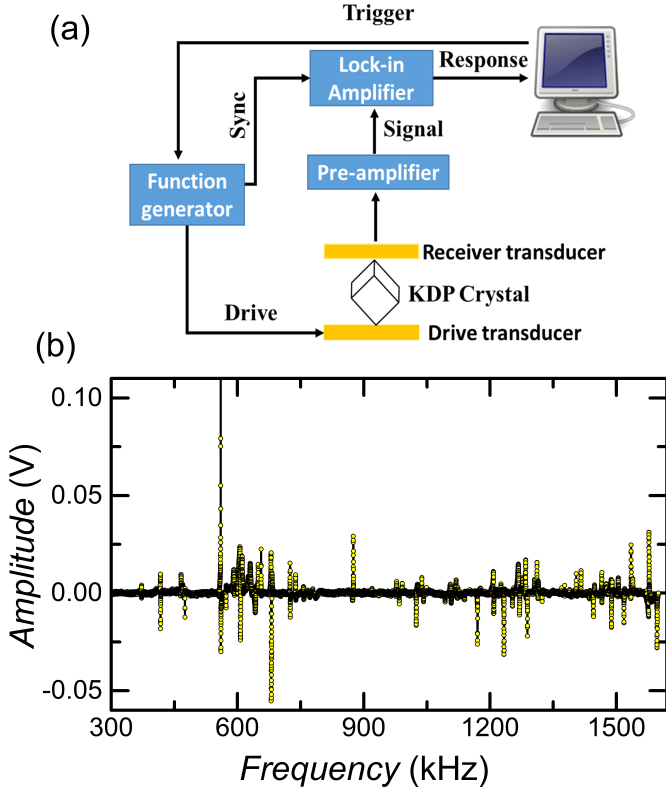


Figure 1: (color online) (a) Schematic of the RUS measurement setup with the KDP crystal mounted between two transducers. (b) Amplitude of the measured RUS spectrum of the KDP crystal, where the peaks correspond to natural elastic resonances of KDP crystal.

2. Experimental Details

Resonant ultrasound spectroscopy (RUS) experiment is performed on high quality KDP single crystal. The single crystal of KDP is grown by slow evaporation of a supersaturated solution method. A rectangular parallelepiped sample is cut along the crystallographic axes and polished with dimensions of $2.3 \times 3.1 \times 2.1 \text{ mm}^3$ and mass density 2288 kg/m^3 . In the RUS experiment, the sample is delicately mounted between two Z-cut LiNbO_3 piezoelectric transducers. One of the transducers functions as the driver and other serves as the signal receiver or detector. To measure the resonances, the drive transducer is excited with a sinusoidal voltage signal of fixed frequency using a function generator (Tektronix AFG 1022) and the sample's response is detected by a Lock-In Amplifier (SRS SR844 RF) through a signal pre-amplifier. A typical schematic diagram is shown in Fig.1(a). The RUS spectrum comprises a series of resonance frequencies that are intricately linked to the elastic constants, dimensions, density, and crystal symmetry of the sample. Resonance arises when the excitation frequency matches with a normal mode of the sample. To obtain a comprehensive set of elastic constants, a substantial number of resonances are indispensable. To capture the large number of resonance modes, excitation frequency is swept from 300 kHz to 1600 kHz and a measured RUS spectrum of KDP single crystal, depicting distinct resonances is shown in Fig.1(b).

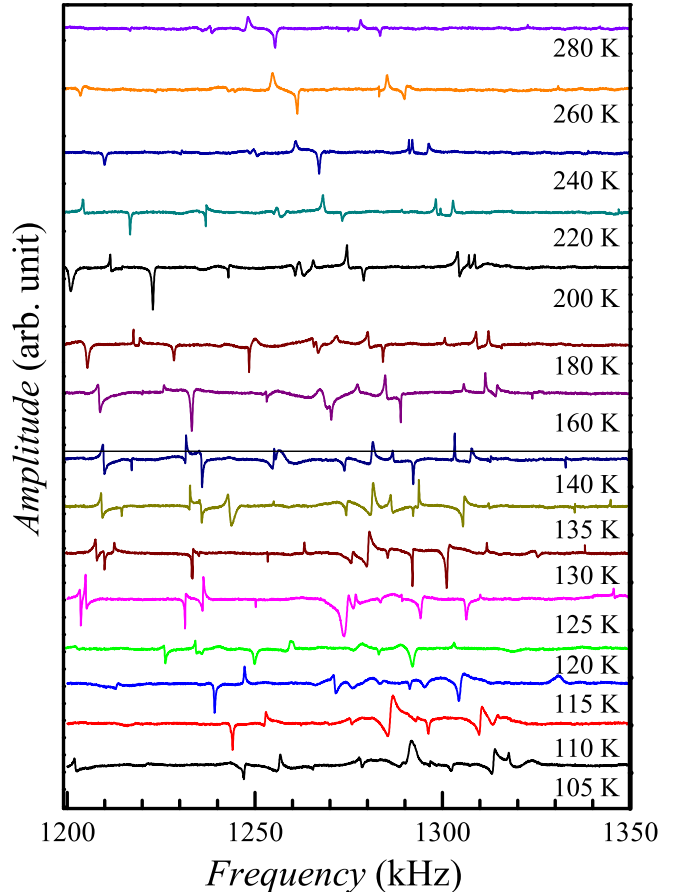


Figure 2: (color online) Temperature-dependent resonant ultrasound spectra of KDP single crystal collected at different temperatures ranging from 280 K to 100 K, covering a frequency range of 1200 kHz to 1350 kHz. To enhance clarity, a y-axis offset is applied, and the measurement temperatures are labeled. Significant variations in the resonance peaks are clearly evident as the temperature changes.

In temperature-dependent measurements, the RUS setup is integrated with a high vacuum compatible variable temperature insert (VTI) that is immersed within a liquid nitrogen Dewar. Precise temperature monitoring and controlling are achieved through a Cernox sensor and a strip heater regulated by a Lakeshore 330 temperature controller. To control the instruments and acquire data seamlessly, we implemented a LabView program. The RUS spectra are acquired over a range of temperatures, spanning from 300 K to 100 K, with a reduced temperature interval of 0.25 K near the phase transition region. Prior to each frequency scan, temperature is well stabilized to within $\pm 10 \text{ mK}$. The analysis of RUS spectra involved employing of the Rayleigh-Ritz method[21, 23, 27, 28]. This method enabled us to determine the natural resonance frequencies by solving the elastic wave equation, taking into account the known elastic constants, dimensions, crystal symmetry, and density of the sample. Further, the least-squares method is utilized to refine the elastic constants by minimizing the difference between the observed and calculated resonances. Through this refinement process, the elastic constants are adjusted iteratively to achieve

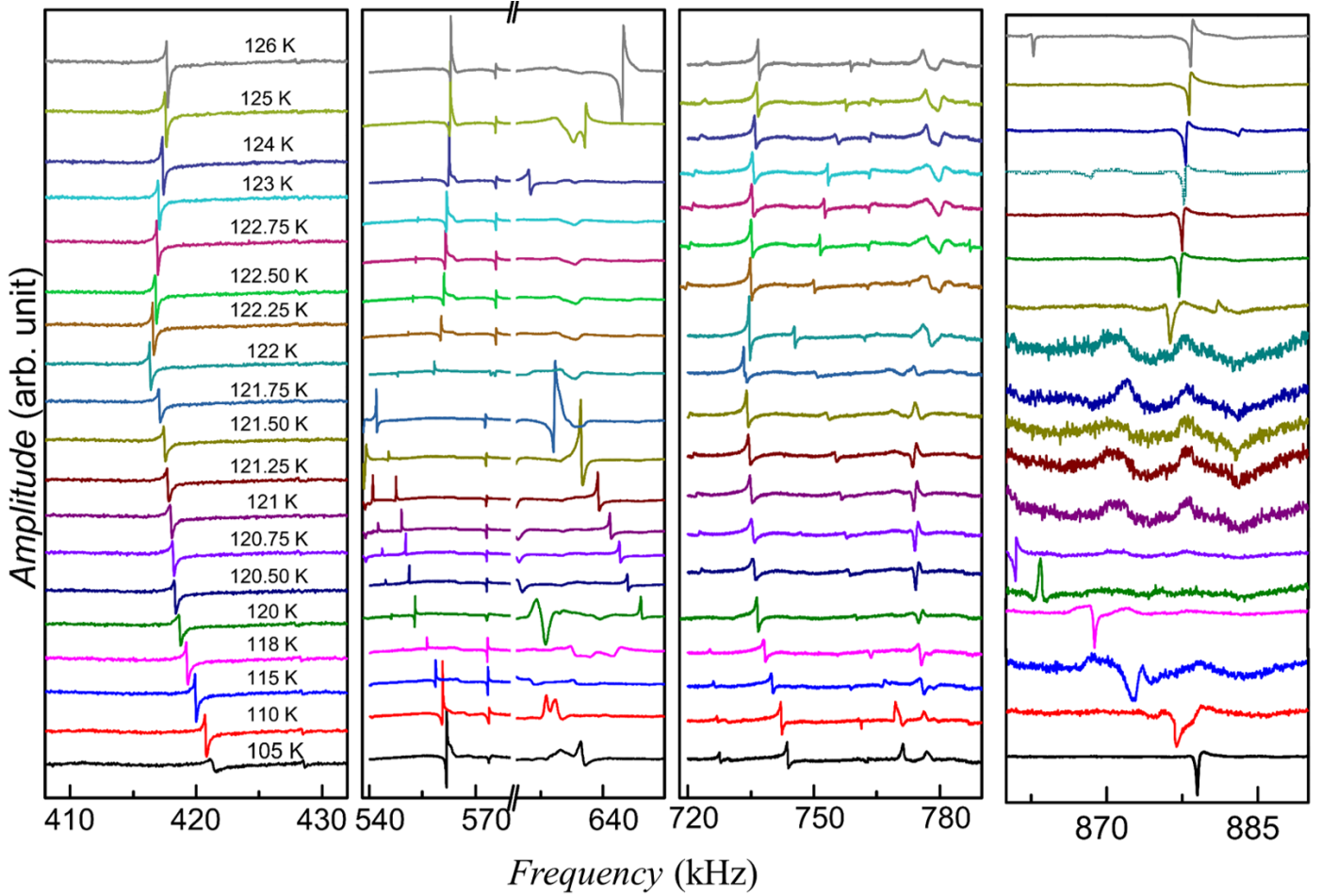


Figure 3: (color online) Temperature-dependent RUS spectra collected within a narrow temperature interval from 126 K to 105 K, across the phase transition. The x-axis is divided into four selected segments, while each spectrum is offset on the y-axis to enhance visualization and clarity. The label indicates the corresponding data collection temperature. A distinct signature of the phase transition is evident in the alteration of resonance peaks.

a better agreement between the experimental and theoretical resonance frequencies.

3. Results and Discussion

Figure 2 illustrates the temperature-dependent RUS spectra, which are acquired within the frequency range of 1200 kHz to 1350 kHz. The spectra are presented with an offset for clarity. Observations reveal a noticeable shift towards lower frequency of the prominent resonances as the temperature increases, indicating elastic softening. However, a significant and abrupt alteration in the resonance pattern is evident across the phase transition temperature. Therefore, to probe the phase transition extensive RUS spectra are measured in the close interval of temperature. Figure 3 represents the RUS spectra, clearly indicating the occurrence of a ferroelectric phase transition. It is observed that certain resonance peaks vanish across the phase transition, signifying a change in the crystal symmetry. Furthermore, some resonances demonstrate elastic softening as the temperature increases, with a subsequent hardening observed at

the transition. To elaborate on this, we have extracted the resonance frequency (f_0), mechanical quality factor ($Q = \Delta f/f_0$) by fitting the resonance peak with the Lorentzian function $A(f) = A_0 \left(\frac{\frac{f}{f_0} \cos \Phi + (1 - (\frac{f}{f_0})^2) Q \sin \Phi}{(\frac{f}{f_0})^2 + (1 - (\frac{f}{f_0})^2)^2 Q^2} \right) + a_1 + a_2 f + a_3 f^2 + a_4 f^3$, where A_0 is the peak amplitude, Q is the quality factor, Φ is the phase and f_0 is the resonance frequency is of the peak and the last term represents a polynomial component incorporated to account the background signal in the fit. Figure 4(a,b) shows the temperature dependent plot of f_0^2 and Q^{-1} obtained from Lorentzian fit of the selected resonances around 417 kHz and 560 kHz. A Lorentzian fit is shown in insert of Fig. 4(a). These resonances initially exhibit a gradual softening as the temperature increases. However, in the vicinity of the ferroelectric transition temperature, a reverse trend characterized by hardening becomes apparent. Following the transition, the softening resumes as the temperature continues to rise. These features can be distinctly observed as the anomalies in both f_0^2 and Q^{-1} around the 122 K. The resonance at 560 kHz demonstrates a notable sensitivity to the ferroelectric to paraelectric phase transition, as it exhibits a pronounced attenuation at the transition

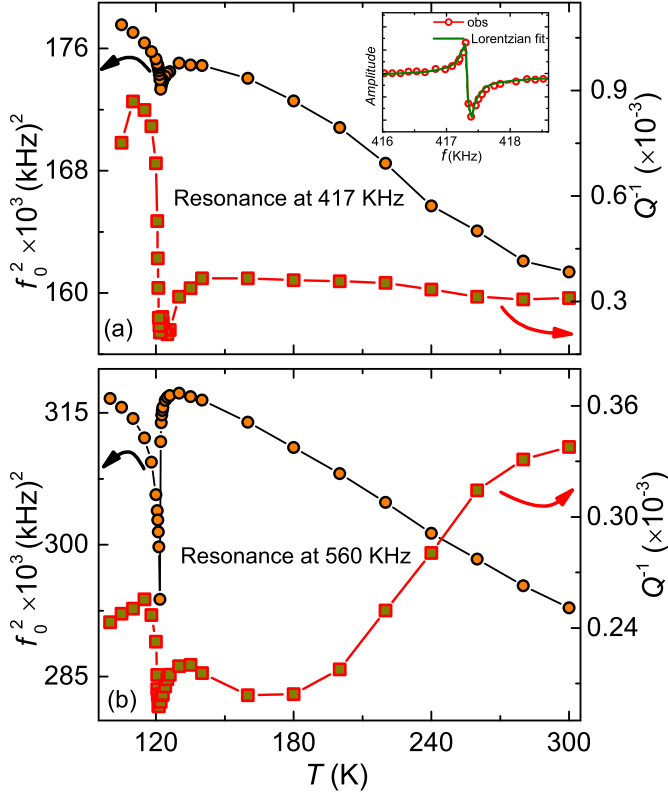


Figure 4: (color online) Temperature dependent of f_0^2 (circle) and Q^{-1} (square) for (a) resonance at 417 kHz and (b) 560 kHz. Inset of (a) contains the Lorentzian fit of corresponding resonance. Note: The error bar is smaller than the size of the symbol.

temperature. The observed strong attenuation indicates the involvement of specific elastic modes associated with the transition.

The elastic constants of KDP are determined through an iterative process, wherein the previously reported values of the elastic constants are used as starting values.[17, 29, 12, 16] As mentioned earlier, KDP exhibits tetragonal crystal symmetry ($\bar{4}2m$) at room temperature, with six distinct elastic constants (C_{11} , C_{33} , C_{44} , C_{66} , C_{12} , C_{13}). However, below 122 K, the crystal symmetry changes to orthorhombic ($2mm$), resulting in nine elastic constants (C_{11} , C_{22} , C_{33} , C_{44} , C_{55} , C_{66} , C_{12} , C_{13} , and C_{23}). In our analysis, the first 60 resonances are selected, and through an iterative procedure, we achieved a difference of $\leq 0.3\%$ between the calculated and observed resonance frequencies (see the supplementary information). The determined elastic constants at 300 K (tetragonal phase) and 100 K (orthorhombic phase) are presented in Table 1. The obtained values of the elastic constants at 300 K are reasonably close to the previously reported for the tetragonal symmetry[17, 29, 12]. The variation of all elastic constants with temperature is plotted in Fig. 5. The observed linear behavior of the elastic constants in the paraelectric phase can be attributed to lattice anharmonicity. However, during the phase transition to the ferroelectric phase, the lattice anharmonicity becomes more pronounced. The presence of spontaneous polarization in the ferroelectric

phase introduces additional interactions and structural changes, causing deviations from harmonic behavior. These deviations manifest as nonlinearities in the elastic response of the material. Across the phase transition, a discontinuity is observed in the elastic constants due to the crystal symmetry change. The elastic constant C_{66} undergoes a significant stiffening of approximately $\sim 27\%$ during the paraelectric to the ferroelectric phase transition, while C_{11} exhibits a softening of $\sim 24\%$ across the transition. Additionally, the off-diagonal constants C_{12} and C_{13} also experience substantial softening throughout this phase transition. In contrast, C_{33} and C_{44} exhibit a minimum value at the transition temperature. It is worth noting that although the absolute values of the elastic constants for tetragonal symmetry align with the reported values, there are noticeable differences in the thermal behavior of these constants across the transition[17, 12]. These disparities in the thermal variations of the elastic constants can be attributed to the explicit consideration of the RUS, which distinguishes it from other ultrasonic methods. The anomalous behavior of elastic constants C_{11} , C_{33} , and C_{66} at the phase transition could be a result of piezoelectric coupling between the lattice and polarization along the Z-direction. On the other hand, the anomalous behavior of the remaining elastic constants C_{12} , C_{13} , C_{44} , and C_{55} suggests the involvement of higher-order piezoelectric coupling mechanisms. Furthermore, the bulk modulus (B) and shear modulus (G) of the KDP crystal are calculated from the Voigt-Reuss-Hill (VRH) approximations[30, 31, 32]. In the VRH approximation, the bulk modulus (B) is determined as the Hill arithmetic average of the bulk Voigt (B_V) and Reuss (B_R) moduli. Similarly, the shear modulus (G) is obtained as the Hill arithmetic average of the shear Voigt (G_V) and Reuss (G_R) moduli. The Voigt and Reuss moduli represent the upper and lower limit of the actual effective moduli, respectively[30, 31, 32, 33]. The relationship of Voigt (B_V and G_V) and Reuss (B_R and G_R) moduli with elastic constants (C_{ij}) for tetragonal and orthorhombic phase can be found in Ref. [34, 33]. The obtained curves for both the bulk modulus (B) and shear modulus (G) are plotted in the inset of Fig.5(f). In this plot, it can be observed that the bulk modulus exhibits a softening behavior, indicating a decrease in stiffness, across the transition. On the other hand, the shear modulus exhibits a minimum value at the transition, suggesting a temporary reduction in resistance to shear deformation.

4. Conclusion

We have investigated the elastic properties of the KH_2PO_4 (KDP) single crystal across the paraelectric to ferroelectric phase transition using the resonant ultrasound spectroscopy (RUS) technique. The paraelectric and ferroelectric phase transition is clearly observed through anomalies in the temperature dependence of resonance frequencies and mechanical quality factor (Q). We have determined the full set of elastic constants for the both tetragonal and orthorhombic phases within the temperature range of 100-300 K. The thermal evolution of the elastic constants exhibits a pronounced change at the transition temperature ($T_C \sim 122$ K). Specifically, the elastic con-

Table 1: Experimentally determined elastic constants (C_{ij}) for KH_2PO_4 (KDP) from RUS data at 300 K and 100 K

System	Elastic constants (GPa)								
	C_{11}	C_{12}	C_{13}	C_{22}	C_{23}	C_{33}	C_{44}	C_{55}	C_{66}
Tetragonal (300 K)	79.32(1)	18.65(3)	9.10(1)	–	–	52.99(2)	13.71(5)	–	6.15(1)
Orthorhombic (100 K)	60.56(2)	4.27(4)	1.58(2)	33.87(2)	14.42(4)	55.54(6)	14.84(3)	4.82(1)	8.77(2)

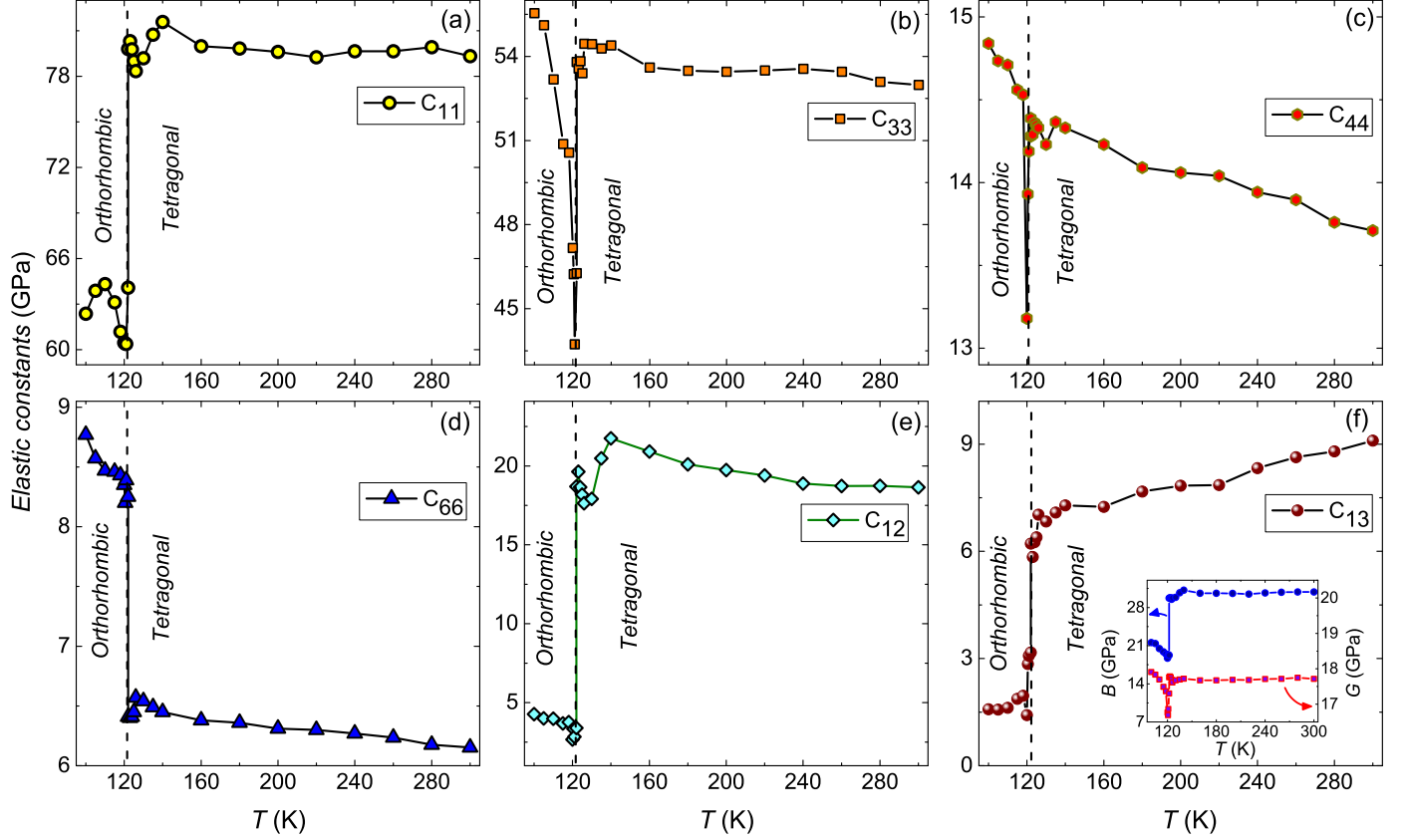


Figure 5: (color online) Temperature dependence of elastic constants (C_{11} , C_{33} , C_{44} , C_{66} , C_{12} , and C_{13}) of KDP single crystal across the tetragonal to orthorhombic phase transition. Inset of (f): Temperature dependence of bulk modulus (B) and shear modulus (G). Note: The error bar is smaller than the size of the symbol.

stants C_{11} , C_{12} , and C_{13} display a significant softening behavior during the transition, while C_{66} experiences a stiffening effect. Additionally, C_{33} and C_{44} demonstrate a minimum value at the transition. The bulk modulus (B) exhibits a sudden softening at the transition, while the shear modulus (G) demonstrates an initial softening followed by stiffening across the transition.

5. Acknowledgements

We would like to acknowledge DST, India for financial support through Grant Number CRG/2019/004653.

References

- [1] C. Salvo, Solid-state light valve, IEEE Transactions on Electron Devices 18 (9) (1971) 748–755. doi:10.1109/T-ED.1971.17276.
- [2] A. Yokotani, T. Sasaki, K. Yoshida, T. Yamanaka, C. Yamanaka, Improvement of the bulk laser damage threshold of potassium dihydrogen phosphate crystals by ultraviolet irradiation, App. Phys. Lett. 48 (16) (1986) 1030. doi:10.1063/1.96638.

- [3] J. J. D. Yoreo, A. K. Burnham, P. K. Whitman, Developing KH_2PO_4 and KD_2PO_4 crystals for the world's most power laser, Int. Mater. Rev. 47 (3) (2002) 113–152. doi:10.1179/095066001225001085.
- [4] W. Reese, L. F. May, Studies of phase transitions in order-disorder ferroelectrics. II. calorimetric investigations of KD_2PO_4 , Phys. Rev. 167 (1968) 504–510. doi:10.1103/PhysRev.167.504.
- [5] J. Kobayashi, Y. Uesu, I. Mizutani, Y. Enomoto, X-ray study on thermal expansion of ferroelectric KH_2PO_4 , Phys. Status Solidi a 3 (1) (1970) 63. doi:https://doi.org/10.1002/pssa.19700030108.
- [6] J. Kobayashi, Y. Uesu, Y. Enomoto, X-ray dilatometric study on ferroelectric phase transition of KH_2PO_4 I. the order of transition, Phys. Status Solidi b 45 (1) (1971) 293–304. doi:https://doi.org/10.1002/pssb.2220450133.
- [7] W. Reese, L. F. May, Critical phenomena in order-disorder ferroelectrics. i. calorimetric studies of KH_2PO_4 , Phys. Rev. 162 (1967) 510–518. doi:10.1103/PhysRev.162.510.
- [8] W. Reese, Studies of phase transitions in order-disorder ferroelectrics. III. the phase transition in KH_2PO_4 and a comparison with KD_2PO_4 , Phys. Rev. 181 (1969) 905–919. doi:10.1103/PhysRev.181.905.
- [9] V. H. Schmidt, A. B. Western, A. G. Baker, Tricritical point in KH_2PO_4 , Phys. Rev. Lett. 37 (1976) 839. doi:10.1103/PhysRevLett.37.839.
- [10] P. Bastie, M. Vallade, C. Vettier, C. M. E. Zeyen, Study of the tricritical point in KH_2PO_4 by γ -ray and neutron diffractometry, Phys. Rev. Lett. 40

- (1978) 337. doi:10.1103/PhysRevLett.40.337.
- [11] F. E. A. Melo, S. G. C. Moreira, A. S. Chaves, I. Guedes, P. T. C. Freire, J. Mendes-filho, Phase diagram uniaxial pressure—temperature of KDP, *Ferroelectrics* 233 (1) (1999) 67. doi:10.1080/00150199908016997.
- [12] A. Petrova, S. Stishov, Elastic properties of KH_2PO_4 at the ferroelectric phase transition, *Solid State Communications* 171 (2013) 26. doi: <https://doi.org/10.1016/j.ssc.2013.07.029>.
- [13] W. P. Mason, The elastic, piezoelectric, and dielectric constants of potassium dihydrogen phosphate and ammonium dihydrogen phosphate, *Phys. Rev.* 69 (1946) 173. doi:10.1103/PhysRev.69.173.
- [14] E. M. Brody, H. Z. Cummins, Brillouin-scattering study of the elastic anomaly in ferroelectric KH_2PO_4 , *Phys. Rev. B* 9 (1974) 179. doi:10.1103/PhysRevB.9.179.
- [15] C. W. Garland, D. B. Novotny, Ultrasonic velocity and attenuation in KH_2PO_4 , *Phys. Rev.* 177 (1969) 971. doi:10.1103/PhysRev.177.971.
- [16] R. F. S. Hearmon, The elastic constants of piezoelectric crystals, *Brit. J. Appl. Phys.* 3 (4) (1952) 120. doi:10.1088/0508-3443/3/4/303. URL <https://dx.doi.org/10.1088/0508-3443/3/4/303>
- [17] E. Litov, C. W. Garland, Ultrasonic experiments in kdp-type crystals, *Ferroelectrics* 72 (1) (1987) 19. doi:10.1080/00150198708017936.
- [18] J. Maynard, Resonant Ultrasound Spectroscopy, *Physics Today* 49 (1) (1996) 26–31. doi:10.1063/1.881483.
- [19] J. D. Maynard, Resonance spectroscopy for solids with layers of different materials, *JASA Express Letters* 2 (12) (2022). doi:10.1121/10.0015316.
- [20] A. Migliori, J. Sarrao, W. M. Visscher, T. Bell, M. Lei, Z. Fisk, R. Leisure, Resonant ultrasound spectroscopic techniques for measurement of the elastic moduli of solids, *Phys. B: Condens. Matter* 183 (1) (1993) 1–24. doi:[https://doi.org/10.1016/0921-4526\(93\)90048-B](https://doi.org/10.1016/0921-4526(93)90048-B).
- [21] R. G. Leisure, F. A. Willis, Resonant ultrasound spectroscopy, *J. Phys. Condens. Matter* 9 (28) (1997) 6001. doi:10.1088/0953-8984/9/28/002.
- [22] B. J. Zadler, J. H. L. Le Rousseau, J. A. Scales, M. L. Smith, Resonant Ultrasound Spectroscopy: theory and application, *Geophys. J. Int.* 156 (1) (2004) 154–169. doi:10.1111/j.1365-246X.2004.02093.x.
- [23] A. Migliori, J. D. Maynard, Implementation of a modern resonant ultrasound spectroscopy system for the measurement of the elastic moduli of small solid specimens, *Rev. Sci. Instrum.* 76 (12) (2005). doi:10.1063/1.2140494.
- [24] F. F. Balakirev, S. M. Ennaceur, R. J. Migliori, B. Maiorov, A. Migliori, Resonant ultrasound spectroscopy: The essential toolbox, *Rev. Sci. Instrum.* 90 (12) (2019). doi:10.1063/1.5123165.
- [25] D. Yang, G. I. Lampronti, C. R. S. Haines, M. A. Carpenter, Magnetoelastic coupling behavior at the ferromagnetic transition in the partially disordered double perovskite $\text{La}_2\text{NiMnO}_6$, *Phys. Rev. B* 100 (2019) 014304. doi:10.1103/PhysRevB.100.014304.
- [26] T. Liu, G. Pei, Z. Zhang, H. Wang, Surface distortion prediction method of KDP frequency converters, in: Y. Huang (Ed.), *Tenth International Conference on Information Optics and Photonics*, Vol. 10964, International Society for Optics and Photonics, SPIE, 2018, p. 10964J. doi:10.1117/12.2506374.
- [27] G. Liu, J. D. Maynard, Measuring elastic constants of arbitrarily shaped samples using resonant ultrasound spectroscopy, *The Journal of the Acoustical Society of America* 131 (3) (2012) 2068. doi:10.1121/1.3677259.
- [28] I. OHNO, Free vibration of a rectangular parallelepiped crystal and its application to determination of elastic constants of orthorhombic crystals, *Journal of Physics of the Earth* 24 (4) (1976) 355–379. doi:10.4294/jpe1952.24.355.
- [29] S. HAUSSÜHL, Elastische und thermoelastische eigenschaften von KH_2PO_4 , KH_2AsO_4 , $\text{NH}_4\text{H}_2\text{PO}_4$, $\text{NH}_4\text{H}_2\text{AsO}_4$ und RbH_2PO_4 , *Z. Kristallogr. Cryst. Mater.* 120 (1-6) (1964) 401. doi:doi:10.1524/zkri.1964.120.16.401. URL <https://doi.org/10.1524/zkri.1964.120.16.401>
- [30] W. Voigt, *Lehrbuch der kristallphysik*: Teubner-leipzig (1928).
- [31] A. Reuss, Berechnung der Fließgrenze von Mischkristallen auf Grund der Plastizitätsbedingung für einkristalle., *Z. Angew. Math. Mech.* 9 (1) (1929) 49–58. doi:<https://doi.org/10.1002/zamm.19290090104>.
- [32] R. Hill, The elastic behaviour of a crystalline aggregate, *Proc. Phys. Soc. A* 65 (5) (1952) 349. doi:10.1088/0370-1298/65/5/307. URL <https://dx.doi.org/10.1088/0370-1298/65/5/307>
- [33] Z.-j. Wu, E.-j. Zhao, H.-p. Xiang, X.-f. Hao, X.-j. Liu, J. Meng, Crystal structures and elastic properties of superhard IrN_2 and IrN_3 from first principles, *Phys. Rev. B* 76 (2007) 054115. doi:10.1103/PhysRevB.76.054115. URL <https://link.aps.org/doi/10.1103/PhysRevB.76.054115>
- [34] T. Gürel, C. Sevik, T. Çağın, Characterization of vibrational and mechanical properties of quaternary compounds $\text{Cu}_2\text{ZnSnS}_4$ and $\text{Cu}_2\text{ZnSnSe}_4$ in kesterite and stannite structures, *Phys. Rev. B* 84 (2011) 205201. doi:10.1103/PhysRevB.84.205201. URL <https://link.aps.org/doi/10.1103/PhysRevB.84.205201>